

Nanoparticles of the Novel Coordination Polymer $\text{KBi}(\text{H}_2\text{O})_2[\text{Fe}(\text{CN})_6] \cdot \text{H}_2\text{O}$ As a Potential Contrast Agent for Computed Tomography

Vindya S. Perera,[†] Jihua Hao,^{§,||} Min Gao,^{*,†} Maya Gough,[†] Peter Y. Zavalij,^{*,†} Chris Flask,^{*,§} James P. Basilion,^{*,§,||} and Songping D. Huang^{*,†}

[†]Department of Chemistry and Biochemistry and [†]Liquid Crystal Institute, Kent State University, Kent, Ohio 44240, United States

[§]Case Center for Imaging Research, Department of Radiology and ^{||}NFCR Center for Molecular Imaging, Case Western Reserve University, Cleveland, Ohio 44106, United States

[‡]Department of Chemistry and Biochemistry, University of Maryland, College Park, Maryland 20742, United States

S Supporting Information

ABSTRACT: An aqueous synthetic procedure for preparing nanoparticles of the novel potassium bismuth ferrocyanide coordination polymer $\text{KBi}(\text{H}_2\text{O})_2[\text{Fe}(\text{CN})_6] \cdot \text{H}_2\text{O}$ is reported. The crystal structure of this coordination polymer is determined through X-ray powder diffraction using the bulk materials. The stability, cytotoxicity, and potential use of such nanoparticles coated with PVP as a CT contrast agent are investigated.

The search for suitable media that can enhance X-ray image contrast began almost immediately after Röntgen discovered X-rays in 1895.¹ Many compounds with elements of high atomic numbers such as bromine, iodine, barium, lead, and bismuth were examined for potential contrast applications, as they have the ability to increase the attenuation of X-rays.² Because of the superior water solubility, versatile synthetic chemistry, and high tolerance by the human body, iodinated organic compounds have dominated the development of X-ray contrast agents for biomedical applications.^{3,4} Today, almost all of the intravascular X-ray contrast agents in computed tomography (CT) are derived from tri-iodinated benzene compounds,^{1–4} although barium sulfate and xenon gas are still used to visualize the gastrointestinal tract and pulmonary system, respectively.⁵ The iodinated organic compounds are characterized by nonspecific extracellular distribution and a short imaging time of approximately 1.5 h due to their rapid clearance by the kidney.^{1,6}

The use of nanoparticles in different imaging modalities represents an important paradigm shift in the development of new-generation contrast agents.^{7–12} Particulate contrast agents can have a greater blood circulation half-life than their molecular counterparts and may be concomitantly detected by multiple imaging modalities.^{13,14} In addition, nanoparticles can penetrate cells and hence are suitable for cellular and molecular imaging applications. Particularly relevant to the development of CT contrast agents drawn on the nanopatform is the ability to derive water dispersible nanoparticles from elements of higher atomic numbers than iodine ($Z = 53$). Recently, nanoparticles of gold ($Z = 79$) were shown to have a higher X-ray attenuation and longer blood circulation times

than iodine-based CT contrast agents.^{15–17} However, given its scarcity and price, gold is more likely to be used in personal ornaments or hidden in vaults than to find its way quickly to CT scanning rooms. On the other hand, the heaviest stable and nonradioactive element with a strong X-ray attenuation power found in the periodic table is bismuth ($Z = 83$).² The latter is considered to be nontoxic compared to its heavy-metal neighbors (e.g., Hg, Tl, Pb) and has a venerable history of applications in cosmetics and medicine.^{18,19} Typical bismuth complexes have a low solubility in aqueous solution or organic solvents.¹⁸ As such, the small-molecule platform has not yet afforded clinically approved bismuth-containing CT contrast agents.² Recently, Weissleder and co-workers demonstrated the efficacy of a polymer-coated Bi_2S_3 nanoparticle preparation as an injectable CT contrast agent.²⁰ Although these nanoparticles exhibit high X-ray adsorption, long circulation times, and excellent imaging efficacy, the *in vivo* hydrolytic stability of such nanoparticles remains unclear.

In this report, we describe a simple one-step aqueous solution route for preparing biocompatible $\text{KBi}(\text{H}_2\text{O})_2[\text{Fe}(\text{CN})_6] \cdot \text{H}_2\text{O}$ nanoparticles. Polyvinylpyrrolidone (PVP) was used as a surface coating agent to control the size and prevent agglomeration of nanoparticles. PVP is a water-soluble and biocompatible polymer that has been used as a blood plasma expander for trauma victims. Various other applications of this polymer are also known in pharmaceuticals and cosmetics.²¹

Slow mixing of 100 mL of aqueous $\text{K}_4[\text{Fe}(\text{CN})_6]$ solution (1 mM) containing 250 mg of PVP (average MW = 8000) with 100 mL of aqueous $\text{Bi}(\text{NO}_3)_3$ solution (1 mM) containing 100 mg of sodium citrate under vigorous stirring resulted in the formation of a homogeneous colorless to pale yellow solution. After acetone was added to this solution, the product was isolated by centrifugation (see Supporting Information). Transmission electronic microscopy (TEM) images of the nanoparticles showed a wide distribution of size from *ca.* 10 to over 30 nm (Figure 1). Distinctive signals for K, Fe, and Bi were detected by energy dispersive X-ray spectroscopy (EDX) analysis (Figure S1), while the atomic ratio of K/Fe/Bi was found to be 1:1:1 in bulk samples by inductively coupled plasma spectroscopy (ICP). The X-ray powder diffraction studies showed that the nanoparticles and

Received: March 22, 2011

Published: July 28, 2011

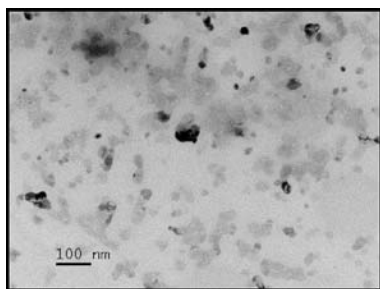


Figure 1. TEM image of BiFeCN nanoparticles.

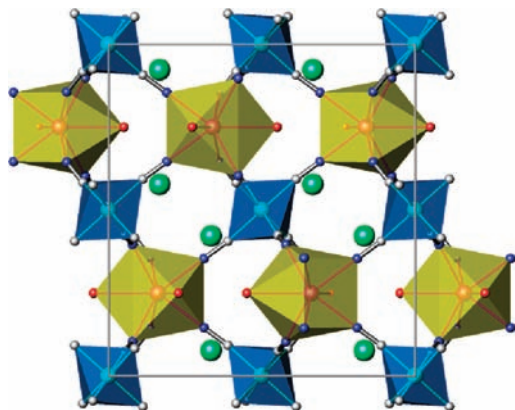


Figure 2. Crystal structure of $\text{KBi}(\text{H}_2\text{O})_2[\text{Fe}(\text{CN})_6] \cdot \text{H}_2\text{O}$ with Bi and Fe shown in yellow and blue polyhedra, respectively. Cyanide ions are shown as thick cylinders (N, blue; C, gray balls). K ions are depicted as large balls.

the bulk sample obtained without the use of PVP are the same phase belonging to a hitherto unknown bismuth cyanide compound.²²

The crystal structure of the title compound was established using X-ray powder diffraction²³ on the bulk sample and found to be isostructural to gadolinium compound of the same stoichiometry.²⁴ Atomic parameters of the latter structure were used as the initial ones in the Rietveld refinement performed using TOPAS software from Bruker. The final refinement (Figure S2) in space group *Pnma* yielded $a = 12.57141(13)$ Å, $b = 13.56839(10)$ Å, $c = 7.26925(9)$ Å, $V = 1239.94(2)$ Å³, and $\rho_{\text{calc}} = 2.72142(5)$ g/cm³ and converged at $R_{\text{Bragg}} = 0.76\%$, $R_{\text{wp}} = 7.04\%$, and $R_p = 7.35\%$.²⁵ The refinement included 36 atomic coordinate and isotropic displacement parameters (Table 1S) refined against 837 reflections within angular range $10 - 110^\circ 2\theta$.

The structure of $\text{KBi}(\text{H}_2\text{O})_2[\text{Fe}(\text{CN})_6] \cdot \text{H}_2\text{O}$ consists of Fe^{2+} octahedra and Bi^{3+} biface-capped trigonal prisms joined in a 3D framework by CN^- groups (Figure 2). The Fe atom is coordinated by six C atoms of the CN^- groups, while Bi is coordinated by six N atoms and additionally by two O atoms of water molecules O1 and O2 (Table 1). The cavities in the framework are filled up by a K^+ ion and water of crystallization (O3), which shows occupation disorder residing in the same cavity. Both K and O3 are slightly shifted from each other by 0.4 Å so that K distances to nearby O and N atoms are in the range of 2.9–3.2 Å, while the O3 water molecule forms two H bonds with O1 and O2 (Table 1).

The Fourier transformed infrared (FT-IR) spectra of the BiFeCN nanoparticles exhibit a strong characteristic $\text{C}\equiv\text{N}$ stretching vibration

Table 1. Selected Interatomic Distances (Å)

atom1	atom2	distance, Å	atom1	atom2	distance, Å
Bi	N1 × 2	2.359(13)	Fe	C1 × 2	1.88(2)
	N2 × 2	2.440(14)		C2 × 2	1.97(3)
	N3 × 2	2.503(13)		C3 × 2	2.02(2)
	O1	2.610(14)	O3	O1	2.66(4)
O2	2.736(15)	O2		2.72(4)	

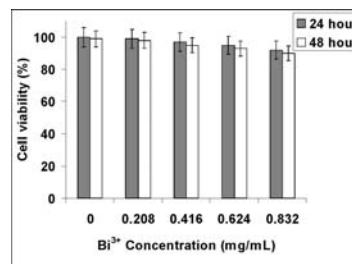


Figure 3. Cell viability curve of BiFeCN nanoparticles.

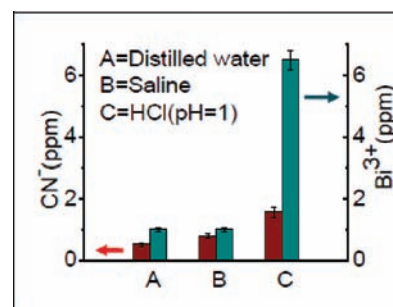


Figure 4. Leaching levels of free CN^- and Bi^{3+} ions.

at 2063 cm^{-1} , in addition to the other characteristic stretching and bending vibrations attributable to PVP (Figure S3).²⁶

The results from thermal gravimetric analysis (TGA) on the bulk sample showed a two-step loss of water before 150°C , which is consistent with the existence of one zeolitic and two coordinative water molecules per formula (Figure S4). We have found that the PVP-coated BiFeCN nanoparticles are stable in solution for over six months.

We studied the cytotoxicity of BiFeCN nanoparticles using a trypan blue exclusion viability assay. Hela cells were incubated for either 24 or 48 h with different amounts of nanoparticles. After 48 h of incubation with a concentration of 0.83 mg/mL, the cell viability was found to be $ca. 90 \pm 4\%$ (Figure 3), indicating that the PVP-coated BiFeCN nanoparticles exhibit no significant cytotoxicity.

We determined the release of free cyanide ions from nanoparticles into solutions using a fluorometric method using the Konig reaction²⁷ and found that the cyanide concentration detected after 24 h of incubation with BiFeCN nanoparticles was below $\sim 0.5 \pm 0.2$ ppm at neutral pH and 1.2 ± 0.2 ppm at $\text{pH} = 1$ (Figure 4). These levels of free cyanide ions are comparable to those found in drinking water or certain plants and fruit seeds or stones.²⁸ The intake of small amounts of cyanide by humans can be rapidly detoxified by the mitochondrial enzyme Rhodanese that converts cyanide into thiocyanate.²⁹ The maximum allowed CN^- contamination level in drinking

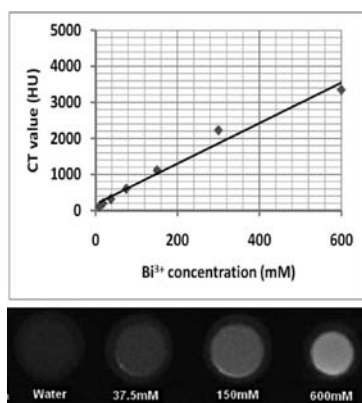


Figure 5. CT intensity values (top) and phantom images (bottom) of nanoparticles with different Bi³⁺ concentrations.

water established by the Environmental Protection Agency (EPA) is 0.2 ppm.³⁰ The elemental analysis using ICP showed that the levels of free Bi³⁺ ions released to the same solutions were below 2 ± 1 ppm at neutral pH and about 7 ± 1 ppm at pH = 1 (Figure 4), while the oral LD₅₀ value of Bi(NO₃)₃ · 5H₂O in the rat was found to be 4042 mg/kg.³¹ The stability of these nanoparticles at such a low pH value is remarkable and suggests the potential of oral delivery of such contrast agents.

We measured the X-ray absorption of nanoparticles at various concentrations. Absorption measurements were obtained as density values in Hounsfield Units (HU). By definition, the density value of water and air is assigned as 0 and -1000 HU, respectively. As shown in Figure 5, a solution of 600 mM PVP-coated BiFeCN nanoparticles has a CT value of 3450 HU. This value is an equivalent X-ray absorption to that of about 1596 mM iodinated contrast agent, indicating that the linear attenuation coefficient of our nanoparticles is ca. 2.7 times of the typical iodine-based CT contrast agent but ca. 62% of the Bi₂S₃ nanoparticles at this concentration.²⁰ The CT value starts to plateau at a concentration of 500–600 mM Bi³⁺. We noticed that the samples of such high concentrations appear slightly cloudy due to the saturation of dispersibility, which causes the data to deviate from a linear fit in this range. These results suggest that the PVP-coated BiFeCN nanoparticles possess potential as a novel CT contrast agent.

In summary, we have discovered an extremely stable and biocompatible nanoplatform to deliver bismuth as a CT contrast agent. Currently, CT is not considered a cellular imaging modality due to the lack of contrast agents that are either cell-permeable or surface-modified with suitable targeting agents that can selectively bind to certain receptors of the cell exterior.³² Our preliminary studies showed that BiFeCN nanoparticles can be internalized by cells *via* endocytosis. Work is under way in our lab to explore cellular imaging and image-guided drug delivery applications of such nanoparticles using the standard clinical CT modality.

■ ASSOCIATED CONTENT

Supporting Information. X-ray crystallographic data in CIF format. Experimental details including synthesis, characterization, and cell viability studies of BiFeCN nanoparticles. This material is available free of charge via the Internet at <http://pubs.acs.org>.

■ AUTHOR INFORMATION

Corresponding Author

*E-mail: shuang1@kent.edu (S.D.H.).

■ ACKNOWLEDGMENT

This work was supported by an OBR-Research Challenge Grant (Grant No. B-9119) from Kent State University and a Summa Health System–Kent State University Research Initiative for Clinical and Translational Research (ICTR).

■ REFERENCES

- (1) Krause, W.; Schneider, P. W. *Topics in Current Chemistry*; Springer: Heidelberg, Germany, 2002.
- (2) Yu, S. B.; Watson, A. D. *Chem. Rev.* **1999**, *99*, 2353–2377.
- (3) Krause, W. *Adv. Drug Delivery Rev.* **1999**, *37*, 159–173.
- (4) Idée, J.-M.; Nachman, I.; Port, M.; Petta, M.; Le Lem, G.; Le Greneur, S.; Dencausse, A.; Meyer, D.; Corot, C. *Top. Curr. Chem.* **2002**, *222*, 151–171.
- (5) Skucas, J. *Radiographic Contrast Agents*, 2nd ed.; Aspen Publishers: Rockville, MD, 1989.
- (6) McClennan, B. L. *Invest. Radiol.* **1994**, *29*, S46–S50.
- (7) Weissleder, R.; Ntziachristos, V. *Nature Med.* **2003**, *9*, 123–128.
- (8) Whitesides, G. M. *Nat. Biotechnol.* **2003**, *21*, 1161–1165.
- (9) Gao, X.; Cui, Y.; Levenson, R. M.; Chung, L. W. K.; Nie, S. *Nat. Biotechnol.* **2004**, *22*, 969–976.
- (10) Alivisatos, A. P.; Gu, W.; Larabell, C. *Annu. Rev. Biomed. Eng.* **2005**, *7*, 1–22.
- (11) Ferrari, M. *Nat. Rev. Cancer* **2005**, *5*, 161–171.
- (12) Rosi, N. L.; Mirkin, C. A. *Chem. Rev.* **2005**, *105*, 1547–1562.
- (13) Lewin, M.; Carlesso, N.; Tung, C. H.; Tang, X. W.; Cory, D.; Scadden, D. T.; Weissleder, R. *Nat. Biotechnol.* **2000**, *18*, 410–414.
- (14) Torchilin, V. P. *Adv. Drug Delivery Rev.* **2006**, *58*, 1532–1555.
- (15) Hainfeld, J. F.; Slatkin, D. N.; Focella, T. M.; Smilowitz, H. M. *Br. J. Radiol.* **2006**, *79*, 248–253.
- (16) Kim, D.; Park, S.; Lee, J. H.; Jeong, Y. Y.; Jon, S. *J. Am. Chem. Soc.* **2007**, *129*, 7661–7665.
- (17) Alric, C.; Taleb, J.; Le Duc, G.; Mandon, C.; Billotey, C.; Le Meur-Herland, A.; Brochard, T.; Vocanson, F.; Janier, M.; Perriat, P.; Roux, S.; Tillement, O. *J. Am. Chem. Soc.* **2008**, *130*, 5908–5915.
- (18) Briand, G. G.; Burford, N. *Chem. Rev.* **1999**, *99*, 2601–2657.
- (19) Sadler, P. J.; Li, H.; Sun, H. *Coord. Chem. Rev.* **1999**, *185*–186, 689–709.
- (20) Rabin, O.; Perez, J. M.; Grimm, J.; Wojtkiewicz, G.; Weissleder, R. *Nat. Mater.* **2006**, *5*, 118–122.
- (21) Bühler, V. *Excipients for Pharmaceuticals-Povidone, Crospovidone and Copovidone*; Springer: Berlin, 2005.
- (22) Dunbar, K. R.; Heintz, R. A. *Prog. Inorg. Chem.* **1997**, *45*, 283–391.
- (23) The experimental diffraction pattern was collected on a Bruker D8 Advance powder diffractometer using Cu K α radiation, a Ni β -filter, and a LynxEye PSD detector. The pattern was measured from 10 to 110° 2 θ with a step size of 0.01446° and an exposition time of 800 s per step; R_{exp} = 2.3%.
- (24) Mullica, D. F.; Ward, J. L.; Sappenfield, E. L. *Acta Crystallogr.* **1996**, *C52*, 2956–2959.
- (25) R_{wp} and R_p calculated with background subtracted.
- (26) Nakamoto, K. *Infrared and Raman Spectra of Inorganic and coordination Compounds Part B: Applications in Coordination, Organometallic and Bioinorganic Chemistry*, 5th ed.; John Wiley & Sons, Inc.: New York, 1997; p 60.
- (27) Yang, Y.; Brownell, C.; Sadrieh, N.; May, J.; Grosso, A. D.; Place, D.; Leutzinger, E.; Duffy, E.; He, R.; Houn, F.; Lyon, R.; Faustino, P. *Clin. Toxicol.* **2007**, *45*, 776–781.
- (28) Vetter, J. *Toxicol.* **2000**, *38*, 11–36.
- (29) Cipollone, R.; Ascenzi, P.; Tomao, P.; Imperi, F.; Visca, P. *J. Mol. Microbiol. Biotechnol.* **2008**, *15*, 199–211.
- (30) See <http://water.epa.gov/drink/contaminants/index.cfm#List> (accessed on March 12, 2011).
- (31) Sano, Y.; Satoh, H.; Chiba, M.; Okamoto, M.; Serizawa, K.; Nakashima, H.; Omae, K. *J. Occup. Health* **2005**, *47*, 293–298.
- (32) Popovtzer, R.; Agrawal, A.; Kotov, N. A.; Popovtzer, A.; Balter, J.; Carey, T. E.; Kopelman, R. *Nano Lett.* **2008**, *8*, 4593–4596.